In vitro fatigue behavior of human dentin with implications for life prediction

R. K. Nalla,[1] V. Imbeni,[1] J. H. Kinney,[2] M. Staninec,[2] S. J. Marshall,[2] R. O. Ritchie[1]
[1]*Materials Sciences Division, Lawrence Berkeley National Laboratory, and Department of Materials Science and Engineering, University of California, Berkeley, California 94720*
[2]*Department of Preventive and Restorative Dental Sciences, University of California, San Francisco, California 94143*

Received 26 April 2002; accepted 23 August 2002

Abstract: Although human dentin is known to be susceptible to failure under repetitive cyclic fatigue loading, there are few reports in the literature that reliably quantify this phenomenon. This study seeks to address the paucity of fatigue data through a systematic investigation of the effects of prolonged cyclical loading on human dentin in an environment of ambient temperature Hank's balanced salt solution (HBSS) at cyclic frequencies of 2 and 20 Hz. The "stress-life" (S/N) data thus obtained are discussed in the context of possible mechanisms of fatigue damage and failure in this material. In addition, stiffness loss data collected *in situ* during the S/N tests are used to deduce crack velocities and the thresholds for such cracking. These results are presented in a fracture mechanics context as plots of fatigue-crack propagation rates (da/dN) as a function of the stress-intensity range (ΔK). Such S/N and da/dN-ΔK data are discussed in light of the development of a framework for a fracture-mechanics-based methodology for the prediction of the fatigue life of teeth. It is concluded that the presence of small (on the order of 250 μm) incipient flaws in human teeth will not radically affect their useful life. © 2003 Wiley Periodicals, Inc. J Biomed Mater Res 66A: 10–20, 2003

Key words: dentin; fatigue; S/N behavior; fractography; sustained-load cracking; fatigue-crack growth; fatigue threshold; life prediction

INTRODUCTION

In human teeth, dentin lies between the exterior enamel and the pulpal soft tissue in the core (Fig. 1); it thus forms the bulk of the interior structure of the human tooth and is critical to its structural integrity. In light of this, it is important that the mechanical properties of dentin be fully characterized in such a way that realistic predictions can be made relative to the effect of microstructural modifications due to caries, sclerosis, and aging on tooth strength, not to mention the effects of various restorative processes commonly employed in dentistry. While several studies have focused on evaluating these properties (see references 1–15), there is very little consistency in the available data.

From a structural viewpoint, exposed root surfaces in teeth often exhibit noncarious notches in the dentin just below the enamel–cementum junction. The etiology for such lesions is believed to involve a combination of erosion, abrasion, and abfraction.[16] While erosion often is the result of exposure to acids, abrasion is caused by the use of inappropriate dentifrice and abfraction by mechanical stresses induced by brushing and chewing. The problem is further complicated by exposure to a wide range of temperatures, chemical compositions, and pH values during intake of food. The notches could serve as very effective stress raisers and often are the sites of failure due to fracture. While cusp fractures are common in posterior teeth, the anterior teeth are more susceptible to fracture at the gingiva, severing the crown of the tooth.

Although such fractures have not been studied extensively, it generally is believed that tooth failure is associated either with catastrophic events induced by very high occlusal stresses or, more plausibly, by cyclic fatigue-induced subcritical crack growth. In view of this possibility, it is perhaps surprising that so few studies have investigated the effect of prolonged fatigue cycling on human dentin, particularly as such information is additionally important for the development of replacement materials for restorative dentistry. To address this deficiency, the present work seeks to present an initial investigation of the response

Correspondence to: R. O. Ritchie; e-mail: RORitchie@lbl.gov
Contract grant sponsor: National Institutes of Health, National Institute of Dental and Craniofacial Research; contract grant number: P01DE09859

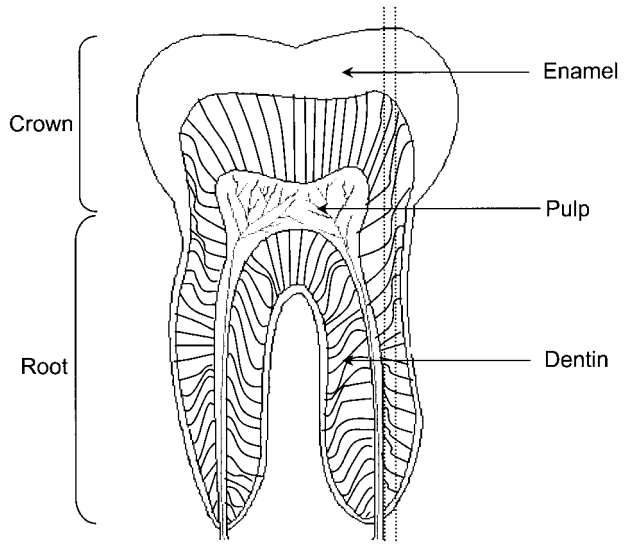

Figure 1. Schematic illustration of a typical human tooth with the section (shown by dotted line) made for the purpose of specimen preparation. Note the tubules running from the dentin–enamel junction towards the pulp in the interior of the tooth.

of dentin to fatigue loading in terms of both classical- (stress-life) and fracture-mechanics-based approaches.

In engineering terms, fatigue refers to the response of a material to repeated application of stress or strain. For most structures, the prediction of a time to failure under such loading conditions is a crucial step for engineering design and the assurance of durability. The classical approach to fatigue has involved the characterization of the total life to failure in terms of a cyclic stress range and often is termed the "stress-life," or "*S*/*N*," approach. This method involves the estimation of the number of cycles required to induce complete fatigue failure of a (nominally flaw-free) "smooth-bar" specimen at a given alternating (σ_a) and mean (σ_m) stress, where the measured fatigue lifetime represents the number of the cycles both to initiate and to propagate a (dominant) crack to failure.

S/*N* curves for certain materials, such as steels, can exhibit a plateau at about 10^6–10^7 cycles, termed the fatigue limit, below which failure does not occur.[17] In the absence of a fatigue limit, a fatigue endurance strength generally is defined as the alternating stress to give a specific number of cycles to failure. Both terms are used as a basis for traditional fatigue design and life prediction, after adjustment for such operational variables as the presence of notches, the environment (e.g., temperature, pH, humidity, etc.), the history and spectrum of loading, etc.[17]

However, in many structures where there is an inherent population of flaws, including human teeth, the crack initiation life may be essentially nonexistent, thus making lifetimes predicted from the *S*/*N* approach highly nonconservative. In these instances, the life may be considered solely as the number of cycles required to propagate one such flaw to failure.

To make such predictions, a fracture mechanics methodology generally is used (termed the damage-tolerant approach), where the number of cycles required for an incipient crack to grow subcritically to a critical size, defined by the limit load or fracture toughness,[18] is computed from information relating the crack velocity to the mechanical driving force (e.g., the stress-intensity factor). For an example of such a "damage-tolerant" life-prediction analysis in the bioengineering context, the reader is referred to the analysis of the projected life of mechanical heart valve prostheses in references 19 and 20.

The specific objective of the present study was to characterize the stress-life and crack-propagation fatigue behavior of human dentin in Hank's balanced salt solution (HBSS) and to use this information as a preliminary basis for developing such lifetime prediction analyses for teeth.

MATERIALS AND METHODS

Materials

Recently extracted human molars were used in this study. Each tooth was sterilized using gamma radiation after extraction.[21] Sections ≈1.5–2.0 mm thick were prepared from the central portion of the crown and the root vertically through the tooth (Fig. 1). The typical microstructure of dentin is shown in Figure 2 and is discussed in the Results section, subsection Microstructure of dentin. Beams of dentin, measuring approximately 0.9 × 0.9 × 10.0 mm, were

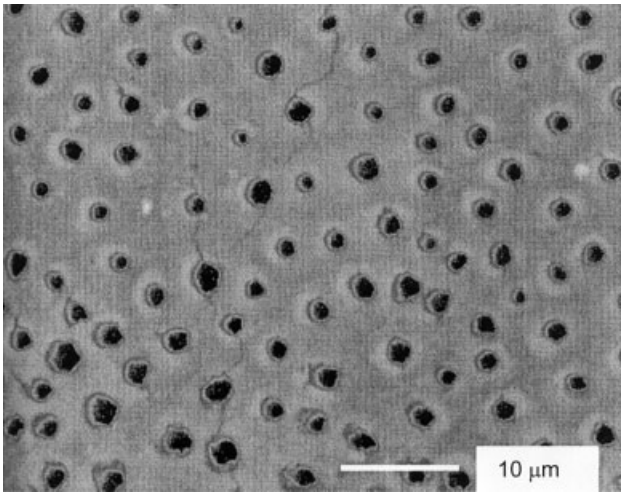

Figure 2. Micrograph illustrating the typical microstructure of human dentin. The most striking feature is the pseudo-periodically placed tubules 1–2 μm in diameter. The orientation of the micrograph is perpendicular to the long axes of the tubules.

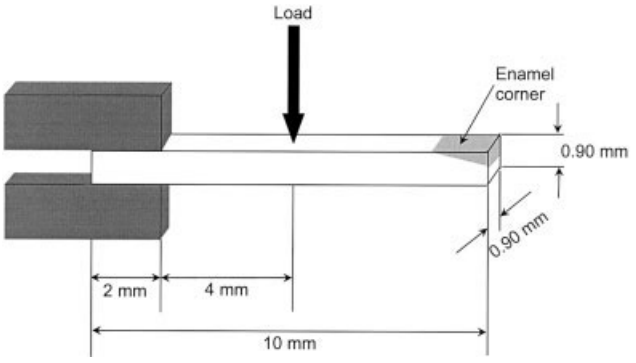

Figure 3. Schematic illustration of the cantilever beam geometry used for *in vitro* fatigue and sustained-load stress-life testing. Each dentin beam tested included some root dentin and some coronal dentin. Testing was conducted in HBSS at ambient temperature.

machined so that the long axes of the tubules were aligned along the lengths of the beams, perpendicular to the plane of the collagen fibrils. In actuality, it is almost impossible *a priori* to align the fracture planes precisely with the tubule axes because, with the exception of the root, the tubules in dentin do not run a straight course from the enamel to the pulp; rather, from the cervical margin through the crown, the tubules have a complex, S-shaped curvature.[22] Consequently, the orientation of the crack plane was determined precisely from examination of the fracture surfaces.

In the present study, all fatigue data were collected on samples where the fracture planes nominally were perpendicular to the average tubule direction. Samples were then obtained from these sections by wet polishing up to a 600-grit finish. Twenty-five such beams were used in the present study. Each beam included some root dentin and some coronal dentin such that the loading configuration shown in Figure 3 could be achieved. *In vitro*, first yield (σ_y) and maximum flexural (σ_F) strength levels were measured in Hank's balanced salt solution (HBSS) in bending to be $\sigma_y \approx 75$ MPa and $\sigma_F \approx 160$ MPa, respectively. It should be noted here that the "yielding" observed could be the result of irrecoverable diffuse damage, as observed, for example, in trabecular bone.[23]

Stress-life testing

In vitro S/N fatigue tests were conducted in ambient-temperature HBSS with unnotched cantilever beams (Fig. 3) cycled on an ELF® 3200 series acoustic testing machine (EnduraTEC Inc., Minnetonka, MN) using a Delrin™ loading rig. Testing was performed at a load ratio, R (minimum load/maximum load), of 0.1 at cyclic frequencies of 2 and 20 Hz. The dentin beams were cycled to failure under displacement control, with the loads being monitored continuously. Stress-life curves were derived for both frequencies in terms of the stress amplitude, σ_a (given by one half of the difference between the maximum and minimum stresses), based on the nominal bending stress in the beam. The minimum and maximum stress levels employed ranged between, respectively, ≈5 and 135 MPa, representing values of ≈3 and 85% of the ultimate tensile strength of the dentin.

In addition, limited stress-life testing also was performed with identical samples under sustained (noncyclic) loads in order to distinguish whether the mechanisms of failure involve processes that are promoted by the maximum rather than the alternating stresses (i.e., static vs. cyclic fatigue). Specifically, specimens were held at a sustained stress level of 118.5 MPa, that is, ≈75% of the ultimate tensile strength, similar to the maximum load used in some of the cyclic fatigue tests, and the time to failure monitored. Unbroken sustained-loaded specimens also subsequently were cycled (at $R = 0.1$ at a frequency of 2 Hz) at an alternating stress of 20 MPa just below the fatigue limit in order to examine the role of crack initiation. Further details of these experiments along with the implications of the results are discussed in the Results section, subsection Sustained-load cracking behavior.

Crack-propagation behavior

Crack-propagation rates were estimated from the loss in stiffness of the test specimens during the S/N fatigue tests. Since the fractography (as described in the Results section, subsection Fatigue-crack propagation behavior) shows that the failure process in dentin involves the initiation and growth of a single dominant crack, continuous *in situ* monitoring of the specimen stiffness, measured in terms of the bending load and loadline displacement, was used to yield an estimate of the specimen compliance, which was then related to a crack size using standard beam theory and fracture mechanics analyses. This method is based on the notion that the extent of local diffuse microdamage around the crack tip is substantially smaller than are all other relevant dimensions. This is akin to the assumption of small-scale yielding in linear-elastic fracture mechanics terminology.

The sample compliance was calculated using the analysis for the additional remote-point displacement, that is, rotation θ_{crack}, due to a crack in a beam under cantilever bending[24]:

$$\theta_{crack} = \theta_{total} - \theta_{no\ crack}, \quad (1)$$

where θ_{total} and $\theta_{no\ crack}$ are, respectively, the total rotation and the rotation of an uncracked sample (of identical dimensions). These rotations readily can be calculated from standard beam theory, where θ_{crack} is given by[24]:

$$\theta_{crack} = 4\sigma S(a/b)/E', \quad (2)$$

where σ is the maximum nominal bending stress (in the absence of a crack), a is the crack length, b is the beam width, $E' = E$, the Young's modulus, in plane stress and $E/(1-\nu^2)$ in plane strain (ν is Poisson's ratio), and the function $S(a/b)$ is given by[24]:

$$S(a/b) = (a/b)^2\{5.93 - 19.69(a/b) + 37.14(a/b)^2 - 35.84(a/b)^3 + 13.12(a/b)^4\}/(1-(a/b))^2. \quad (3)$$

Through continuous monitoring of this change in compliance, the crack length, a, and hence the crack-growth rate, da/dN, was determined. Crack-growth rates were computed using finite-difference methods over increments of crack extension of approximately 70 μm.

With a knowledge of the applied loads and the crack length, the stress-intensity factor, K, can be determined; this parameter characterizes the magnitude of the stress and displacement fields ahead of the crack, and as such can be used to describe the linear-elastic driving force for crack advance. In the present study, stress intensities were calculated from standard handbook solutions, in terms of the applied stress range, $\Delta\sigma$, and crack size, a[24]:

$$\Delta K = -\Delta\sigma(\pi a)^{1/2} f(a/b)\,, \quad (4)$$

where ΔK is the stress-intensity range ($= K_{max} - K_{min}$), and $f(a/b)$ is a function of the specimen geometry and crack size,[24,25] viz.:

$$f(a/b) = 1.122 - 1.40(a/b) + 7.33(a/b)^2 - 13.08(a/b)^3 + 14.0(a/b)^4\,. \quad (5)$$

The crack propagation results are presented as standard log–log plots of the growth rate per cycle, da/dN, as a function of the stress-intensity range, ΔK.

Fractography

The morphologies of the fracture surfaces for both fatigue and overload fractures were examined using a standard scanning electron microscope. Surfaces were sputter-coated with a gold-palladium alloy prior to investigation. In addition, the crack paths were examined by stopping a test specimen containing a growing fatigue crack prior to failure and examining it metallographically perpendicular to the plane of the fracture surface. To achieve this, the section of the specimen containing the crack was cold-mounted in epoxy, polished down to a 1200-grit finish, and sputter-coated prior to investigation by optical and scanning electron microscopy.

RESULTS

Microstructure of dentin

Human dentin essentially is a hydrated composite composed of nanocrystalline carbonated (calcium-phosphate-based) apatite mineral (≈45% by volume), type-I collagen fibrils (≈30% by volume), fluid, and other noncollagenous proteins (≈25% by volume). The apatite mineral is distributed in the form of fine crystallites (5 nm thick) in a scaffold created by the collagen fibrils (typically 50–100 nm in diameter).

The distinctive feature of the "microstructure" of the dentin is a distribution of cylindrical tubules (typically ≈1–2 μm in diameter) that run from the dentin–enamel junction to the interior pulp chamber (Figs. 1 and 2). These dentinal tubules are surrounded by a collar of highly mineralized peritubular dentin (≈1 μm thick) and are embedded within a matrix of mineralized collagen called intertubular dentin. The mineralized collagen fibrils form a planar felt-like structure oriented perpendicular to the tubules.[26] The tubules can be considered to be randomly displaced about a periodic lattice,[27] but with a distribution that depends on location within the tooth.

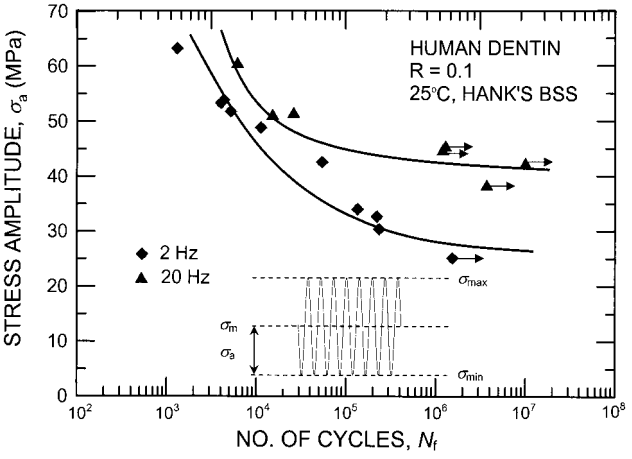

Figure 4. Stress-life (S/N) data for dentin in HBSS in the form of the stress amplitude, σ_a, as a function of the number of cycles to failure, N_f. Results were obtained at frequencies of 2 and 20 Hz, with a load ratio of $R = 0.1$. Horizontal arrows represent samples that did not fail. The inset shows the definition of the various stresses associated with the fatigue cycle.

There is evidence, although somewhat inconclusive, that the orientation of the tubules leads to anisotropic mechanical properties in human dentin (e.g., see Refs. 5,6, and 12). Similar directional anisotropy has been reported for other biologic tissues, for example, bone (see Ref. 28). The present study, however, is restricted to a single orientation, with cracking nominally perpendicular to the long axis of the tubules, that is, in the plane of the collagen fibrils. This orientation is believed to have the lowest fracture toughness properties.[5,6,8,18]

Stress-life behavior

Stress-life data, obtained at cyclic frequencies of 2 and 20 Hz with $R = 0.1$, are shown in Figure 4 and Table I in the form of the number of fatigue cycles to failure, N_f, as a function of the applied stress amplitude, σ_a. Results are compared with corresponding behavior under sustained loading. Each reported lifetime is from a single specimen. Cyclic fatigue data spanning about five decades in life, from 10^2–10^3 to

TABLE I
Stress-Life and Stress-Time Data For Fatigue and Sustained-Load Cracking (SLC) in Human Dentin

Stress Amplitude σ_a (MPa)	Cycles to Failure N_f	Maximum Stress σ_{max} (MPa)	Time to Failure t_f (s)
2 Hz:			
63.3	1.30×10^3	139.0	6.50×10^2
53.9	4.30×10^3	118.5	2.15×10^3[a]
53.3	4.00×10^3	118.5	2.00×10^3
51.9	5.16×10^3	118.0	2.00×10^3
48.9	1.12×10^4	108.6	2.56×10^3
42.6	5.41×10^4	97.5	2.70×10^4
34.1	1.35×10^5	75.7	6.75×10^4
32.7	2.22×10^5	72.7	1.11×10^5
30.5	2.35×10^5	70.8	1.18×10^5
25.2	$>1.54 \times 10^6$	56.0	$>7.70 \times 10^5$[b]
20 Hz:			
60.7	6.10×10^3	135.4	3.05×10^2
51.3	1.51×10^4	109.7	7.56×10^2
51.7	2.60×10^4	114.8	1.30×10^3
44.9	$>1.20 \times 10^6$	99.7	$>6.00 \times 10^4$[b]
45.7	$>1.29 \times 10^6$	101.2	$>6.45 \times 10^4$[b]
42.5	$>10.0 \times 10^6$	97.5	$>5.00 \times 10^5$[b]
38.5	$>3.72 \times 10^6$	88.3	$>1.86 \times 10^5$[b]
SLC Test B (see Fig. 5):			
0	—	118.5	$>2.38 \times 10^5$[b]
SLC Test C (see Fig. 5):			
20	$>1.72 \times 10^6$	44.4	$>8.59 \times 10^5$[b]

[a]Test A (see Fig. 5).
[b]Specimen did not fail

10^6–10^7 cycles, were obtained. It is evident that dentin shows "metal-like" fatigue behavior in that fatigue lifetimes increase with decreasing stress amplitudes until an apparent plateau, resembling a fatigue limit, is reached at $\approx 10^6$ cycles. Values for this apparent fatigue limit in dentin ranged from 25 MPa at 2 Hz to 45 MPa at 20 Hz, representing values of ≈15 to 30% of the measured tensile strength. This is to be compared with most metallic materials where, at this load ratio, the fatigue limit typically is 25 to 30% of the tensile strength.

There is a marked effect of cyclic frequency on the stress-life fatigue behavior of human dentin, with substantially longer lifetimes at the higher frequency. This effect has been observed in many systems, for example, in human bone,[29] bone cement,[30] and in many metallic materials,[17] and generally is attributed either to a time-dependent contribution to cracking (e.g., at lower frequencies the crack is open for a longer time period, thus permitting environmentally assisted cracking mechanisms to be more active) or, in rarer cases, to strain-rate effects.[17]

If the data in Figure 4 are re-plotted on the basis of time rather than cycles, where the maximum applied stress, σ_{max}, is plotted as a function of the time-to-failure, t_f, (Fig. 5), the effect of testing frequency is significantly diminished, indicating that the mechanisms of fatigue-related failures in dentin may be predominantly time, rather than cycle, dependent. Similar behavior previously has been reported in human bone.[29]

Crack path and fractographic observations

The fractography of fatigue and overload (fast fracture) failures in human dentin is shown in the scanning electron micrographs in Figures 6–8. A low-magnification view of the entire fracture surface of a cyclic fatigue sample, shown in Figure 6, indicates that crack initiation occurred at the top surface of the sample (between the two white arrows), where the tensile stress is at a maximum. Subsequent fatigue-crack growth was relatively free of tortuosity and occurred in a plane perpendicular to the long axis of the tubules.

Higher magnification images of the fatigue region in Figure 7 reveal little evidence of a marked effect of the tubules in influencing the crack-advance process, as might be seen, for example, by cavitation or the "bowing" of the crack front around the tubules. There may have been some degree of pullout of the peritubular dentin cuffs surrounding the tubules (as indicated by the arrows in Figs. 7 and 8), which could have contributed to the crack-growth resistance. However, there was no evidence of fatigue striations, which are indicative of an incremental crack-growth process re-

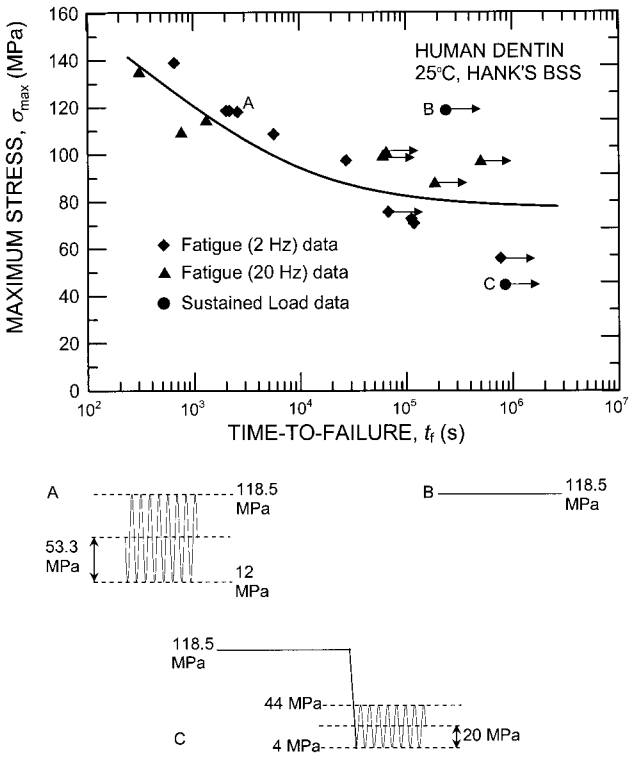

Figure 5. Stress-time data for dentin in HBSS in the form of the maximum stress, σ_{max}, as a function of the time to failure, t_f. Results were derived from those in Figure 4 together with the results of two sustained-load tests. Horizontal arrows represent samples that did not fail. The schematics illustrate the stress levels and sequences used for these tests.

sulting from alternating plastic blunting and sharpening at the crack tip. This process represents the most common fatigue mechanism in ductile materials, such as many metals and polymers,[17] but apparently is not operating in human dentin.

Fracture surfaces representative of the overload failure are shown in Figure 8. As reported previously,[31] few differences exist between the morphology of these fractures and those associated with cyclic fatigue-crack growth (Fig. 7) although macroscopically the overload fracture surfaces are somewhat rougher. Such behavior is more indicative of brittle materials, such as many ceramics and pyrolytic carbon,[31,32] where the mechanisms of crack advance (and hence the fractography) essentially are identical under cyclic and overload conditions; the fatigue effect in these materials more commonly is associated with mechanisms behind the crack tip, involving the progressive degradation of the operative crack-tip shielding (extrinsic toughening) processes.[33] Furthermore, there were no observable differences in the appearance of the fracture surfaces at 2 Hz and at 20 Hz.

A typical scanning electron micrograph of the crack profile is included in Figure 9. As is evident, there is very little tortuosity in the path that the fatigue crack follows, indicating that the tubule-based microstructure does not appear to significantly influence the propagation of the crack and hence does not appear to contribute to the toughness or fatigue resistance. However, there is some evidence of pull-out of the peritubular dentin cuff inside the crack, as indicated by the white arrows in the figure, which may be indicative of a small contribution to the crack-growth resistance.

Sustained-load cracking behavior

It is evident from the fatigue results in Figure 5 that plotting with respect to time provides a somewhat better representation of the data. This raises the possibility that the primary mechanism of subcritical crack growth in dentin is time, rather than cycle, dependent. Such sustained-load cracking (SLC) mechanisms often are environmentally assisted, for example, stress-corrosion cracking, and commonly are encountered in the fatigue of brittle materials where the cycle-dependent mechanisms are less prevalent. Indeed, it is well known that fatigue lifetimes can be predicted from static fatigue data for such materials, in the absence of any cycle-dependent mechanisms.[34,35]

Using this analysis in reverse, which equates the role of static and cyclic loads by integrating over the fatigue loading cycle, the time to failure under static loading, t_s, can be related to the corresponding time to failure under cyclic loads, t_c, in terms of the relative

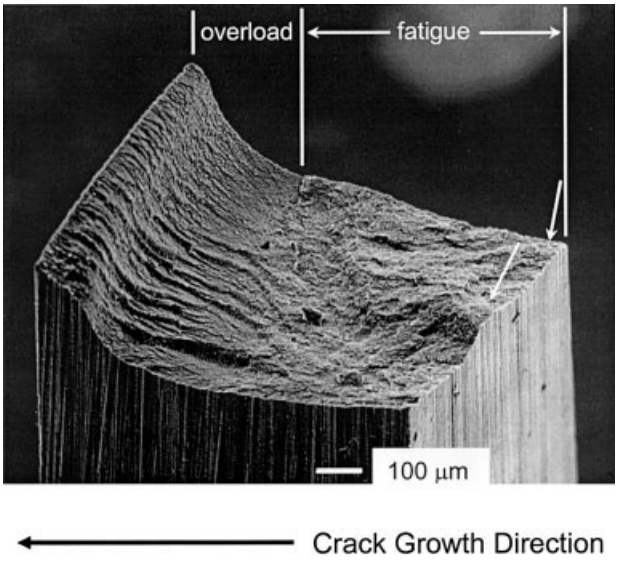

Figure 6. Low magnification scanning electron micrograph of a failed stress-life fatigue sample, showing the probable fatigue crack initiation site (indicated by white arrows) on the top surface where the tensile stresses are at a maximum. The extension of the fatigue crack proceeds from right to left until catastrophic failure occurs.

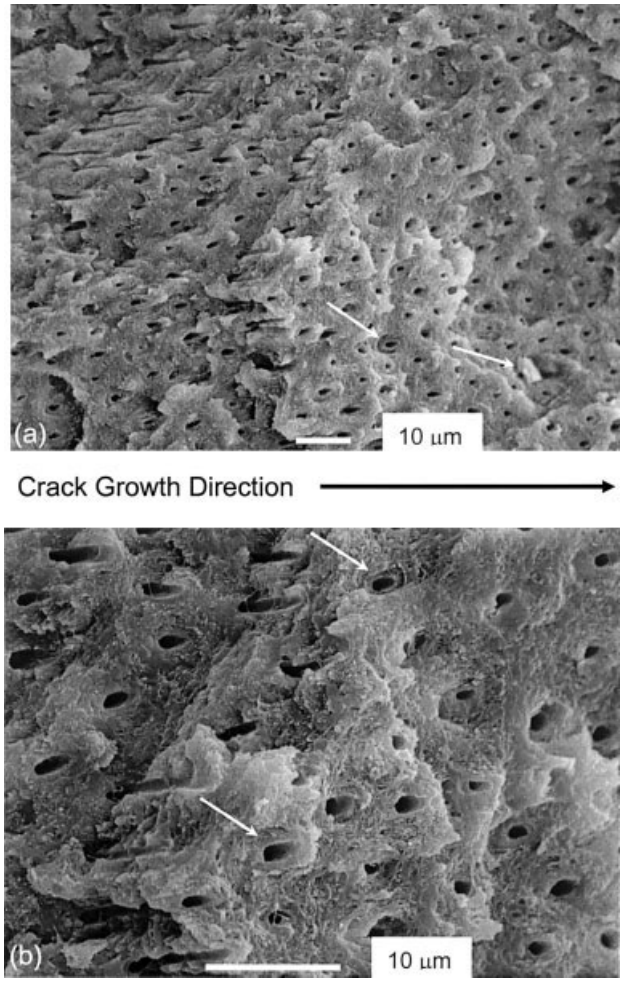

Figure 7. Higher magnification scanning electron micrographs of the cyclic fatigue region of the fracture surface, showing evidence of pullout of the peritubular dentin cuffs (indicated by white arrows). The nominal direction of crack growth is from left to right.

magnitudes of the stress amplitude, σ_a, in the fatigue test and the corresponding maximum stress, σ_s, in the static test[34]:

$$t_s/t_c = g(\sigma_a/\sigma_s)^n \quad (6)$$

where n is an environment- and temperature-dependent system constant (typically 15 to 60) and g is the time-to-failure ratio (from Ref. 34).

Using results at a stress level of 118.5 MPa, representing the maximum stress corresponding to a fatigue stress amplitude of σ_a = 53.3 MPa, where the experimentally measured fatigue lifetime was 4000 cycles at 2 Hz (Fig. 5), Equation (6) implies that the time to failure under static loads should be in the range of 180 to 460 s. However, experimentally, no failures were observed even after $\approx 2.4 \times 10^5$ s at a sustained load of 118.5 MPa. There are several explanations for this apparent inconsistency: (1) there are both time- and cycle-dependent mechanisms that are active during the fatigue of dentin in physiologic environments (which is very likely), and (2) crack initiation occurs much more readily under cyclic loading.

To examine this latter point further, one specimen tested under sustained loading subsequently was fatigue cycled at 20 MPa, just below the fatigue limit (at $R = 0.1$ with 2 Hz of frequency). Once again, no failure was observed even after over 1.72×10^6 cycles ($\approx 8.6 \times 10^5$ s). This experiment implies that a crack had not initiated under sustained loading even after more than 10^5 s at a load level at which under cyclic loading, failure would have ensued in less than 2000 s. This strongly suggests that the process of crack initiation in human dentin is far more difficult under sustained loading, compared to that under corresponding cyclic loads. Similar behavior is observed in many lower-strength metallic materials, where the thresholds for

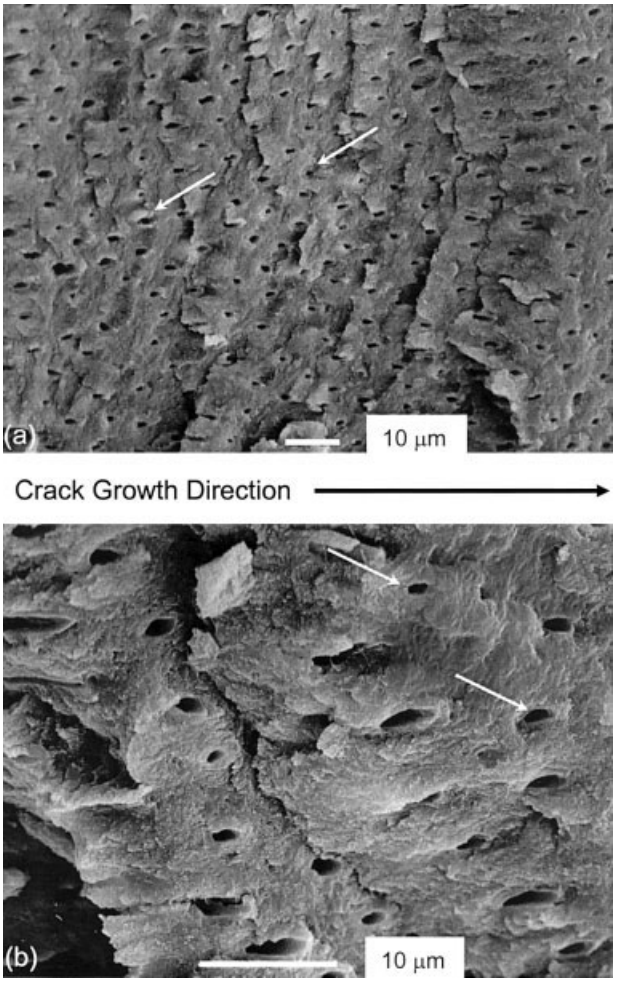

Figure 8. Corresponding scanning electron micrographs of the overload fracture region of the fracture surface. Although this fracture surface is macroscopically "rougher" than that of the fatigue fracture surfaces, the morphology is essentially identical. Some evidence of pullout of the peritubular dentin cuffs (indicated by white arrows) again can be seen. The nominal direction of crack growth is from left to right.

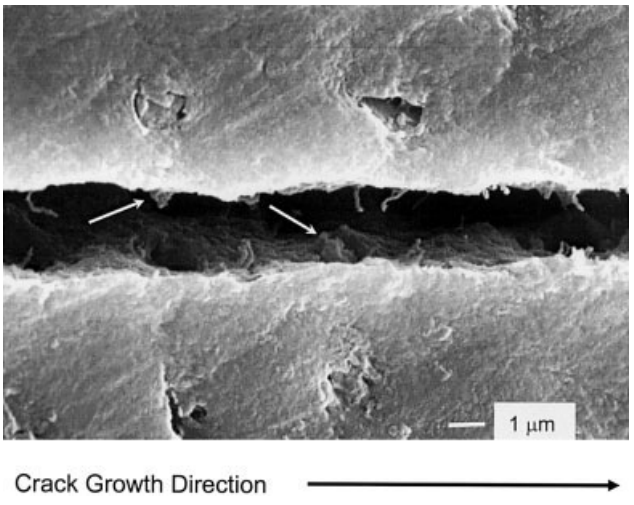

Figure 9. Scanning electron micrograph of a typical crack path of a fatigue crack through the dentin microstructure. Note the small degree of pullout of the peritubular dentin, as indicated by the white arrows inside the crack.

subcritical cracking are much lower in cyclic loading than under sustained loads.[36]

Fatigue-crack propagation behavior

To the authors' knowledge, there are no reports to date of fatigue-crack propagation behavior for human dentin in archival literature. In the present study, such data were derived from continuous *in situ* measurements of stiffness loss during S/N fatigue tests; typical plots of the drop in maximum load, at constant displacement, in the fatigue cycle with the number of cycles are shown in Figure 10. It is apparent that the decay in stiffness is relatively minor until the latter stages of the test, indicating that, similar to many materials, the majority of the fatigue lifetime is spent in initiating a small propagating crack (in this instance, typically on the order of 100–150 μm).

Using the procedures described in the Materials and Methods section, subsection Crack-propagation behavior, to estimate the crack lengths, stress-intensity levels, and crack-growth rates, a plot of the variation in da/dN with the stress-intensity range ΔK was derived. The results are shown in Figure 11 and are believed to be the first reported fatigue-crack growth rate data for human dentin. In common with many materials,[17] the variation in growth rates with ΔK in dentin can be described by a simple Paris power-law relationship:

$$da/dN = C(\Delta K)^{m} = 6.24 \times 10^{-11}(\Delta K)^{8.76} \qquad (7)$$

where C and m are scaling constants, with their values quoted for units of MPa$\sqrt{}$m (on ΔK) and m/cycle (on da/dN). This behavior is consistent with that observed for many brittle materials, which usually have far higher Paris exponents than the m values of ≈2 to 4 that generally are reported for ductile (e.g., metallic) materials.[33] The exponent of ≈8.76 found for dentin is somewhat smaller than that reported for apatite bone mineral substitute (where m is ≈17).[37]

When characterizing the fatigue-crack growth properties of a material, it often is useful to define a threshold stress intensity, ΔK_{TH} or $K_{max,TH}$, below which crack growth is dormant or proceeds at vanishingly low rates; this parameter can be defined operationally as the stress intensity corresponding to an average growth rate of 10^{-10} m/cycle. Extrapolating the current results to this lower bound yields an approximate threshold ΔK_{TH} for human dentin of 1.06 MPa$\sqrt{}$m. This value is roughly 60% of the measured fracture toughness [K_c ≈1.8 MPa$\sqrt{}$m (Ref. 18)] and is typical of many brittle materials where ΔK_{TH} is ≈0.4–0.6 K_c.[33] By comparison, fatigue thresholds for other common brittle materials are in the same range: ΔK_{TH} ≈2.5 MPa$\sqrt{}$m for cortical bone,[37,38] ≈1 to 4 MPa$\sqrt{}$m for

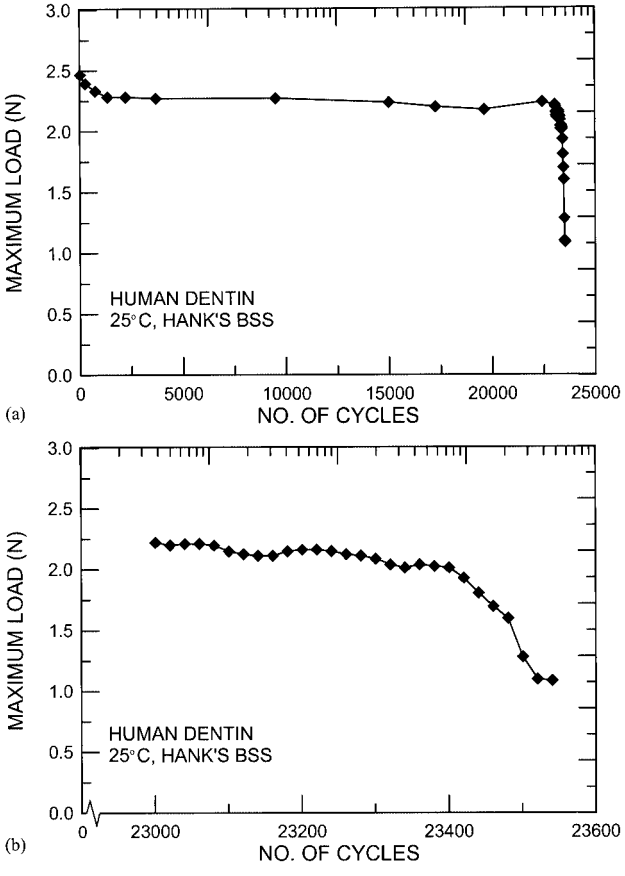

Figure 10. Typical stiffness-loss data obtained during a stress-life test, showing the drop in maximum load at constant displacement as a function of (a) the number of loading cycles. The stiffness is relatively constant for the majority of the test, until (b) it drops significantly near the end. This implies that the majority of the life is spent in initiating a growing crack.

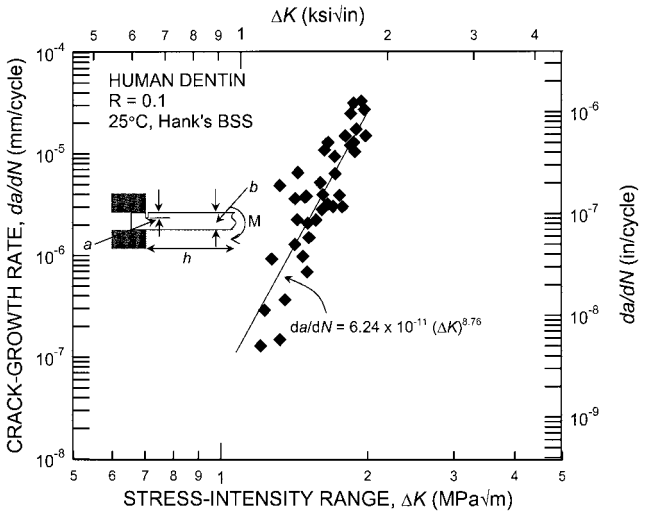

Figure 11. Plot of the variation in fatigue-crack growth rates, *da/dN*, with the stress-intensity range, ΔK, for human dentin in HBBS at $R = 0.1$. The results suggest a simple Paris power-law relationship, with an exponent of m ≈8.7, for crack-growth behavior. The inset shows an illustration of the geometrical configuration used for these calculations.

alumina (depending upon grain size),[33] and ≈0.6 to 0.8 MPa√m for pyrolytic carbon.[32]

It should be noted that the threshold of 2.5 MPa√m, reported in reference 37, was taken from the data for adult bovine bone described in reference 38. However, as no attempt was made to actually measure the threshold in reference 38 and the growth rates reported are no lower than 10^{-7}–10^{-6} m/cycle, it is likely that the actual threshold for this material is significantly lower than the result quoted in reference 37.

DISCUSSION

Typical masticatory stress levels that a human tooth experiences have been estimated to be on the order of 20 MPa.[39] Although these stresses generally are due to compressive loading, at these levels a measured fatigue threshold for dentin of ≈1 MPa√m implies that any cracks formed in teeth would need to be of dimensions in the hundreds of micrometers before meaningful subcritical crack growth could occur.

With the availability of the growth-rate data for dentin shown in Figure 11, it is now possible to make a preliminary attempt to develop conservative estimates of the expected fatigue life of teeth containing flaws of specific dimensions. This "lifing" procedure uses a worst-case fracture mechanics approach that is based on the notion that the lifetime is comprised of the time or number of loading cycles for the largest pre-existing flaw to propagate to a critical size where catastrophic failure occurs. This is achieved by integrating the Paris crack-growth relationship [Eq. (7)] between the limits of the initial flaw size, a_o, and the critical (final) flaw size, a_c, for failure. The latter limit can be estimated by equating the stress intensity developed ahead of the crack tip to the fracture toughness, K_c:

$$K = f(a/b)\sigma_{app}(\pi a_c)^{1/2} = K_c\,, \tag{8}$$

where σ_{app} is the in-service stress, $f(a/b)$ is a function dependent upon the geometry, flaw size and shape, and K_c for dentin is ≈1.8 MPa√m.[18] The number of loading cycles needed to cause failure thus is a strong function of the in-service stress and initial flaw size and can be expressed (for $m \neq 2$) as:

$$N_f = \frac{2}{(m-2)C}\,(f(a/b)\Delta\sigma_{app})^{-m}\pi^{-m/2}[a_o^{1-m/2} - a_c^{1-m/2}]\,, \tag{9}$$

thereby providing a conservative basis for the prediction of the life of a tooth. Since the scaling constants C and m are set by the crack-growth relationship for dentin in Equation (7), and we can reasonably assume masticatory stress levels of ≈20 MPa,[39] the principal factor that needs to be defined is the function $f(a/b)$, which usually is of the order of unity but depends specifically on the size and shape of the flaw and its configuration within the tooth.

As an illustration of this approach, we can assume the presence of a semi-elliptical surface flaw that is small compared to the dimensions of the tooth. For shallow cracks in this configuration, $f(a/b) = 1.12/\sqrt{\Phi}$, where Φ is the so-called shape factor (an elliptic integral of the second kind that depends upon the shape of the flaw and the level of stress in relation to the flow stress).[40] Since the in-service stresses generally are small ($\sigma_{app}/\sigma_{uts} \approx 0.12$), a worst-case value for Φ for a shallow crack can be taken as 1. Using this configuration for Equation (9), predictions of the life as a function of the initial flaw size are shown in Figure 12 for a range of in-service stress levels.

As noted above, because of the moderately high Paris exponent ($m \approx 8.76$) in dentin (as compared to most metallic alloys), projected lives are a very strong function of initial flaw size. Specifically, for an initial flaw of ≈100 μm in size, the predicted fatigue lifetime at a worst-case stress of 20 MPa is well over a billion cycles. On the assumption that a human tooth is subjected to something on the order of a million cycles per year,[41] the fatigue life of the tooth would be infinite. However, for a larger flaw of 600 μm in size, the projected life drops to ≈3.6 million cycles, or 3 to 4 years; for a 900-μm flaw, the projected life is as low as a few months. One implication of this is that any dental reconstruction process that leaves, for example, a millimeter-sized flaw, would mean that the residual

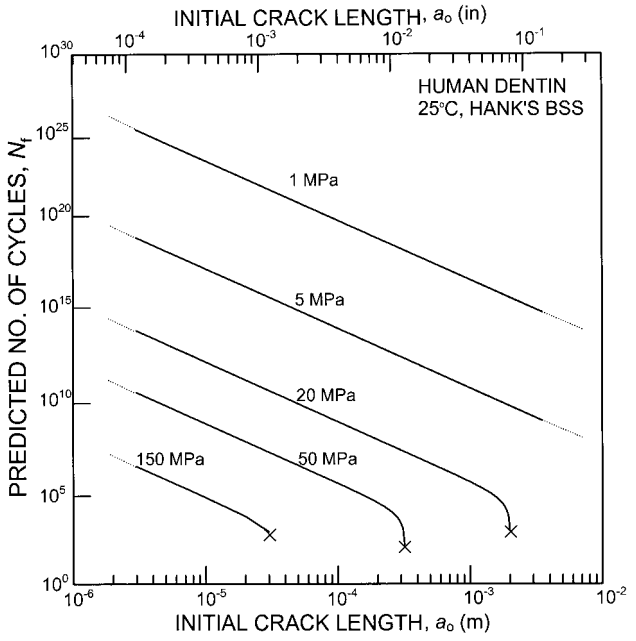

Figure 12. Predicted fatigue lives in terms of the number of loading cycles, N_f, and as a function of the initial flaw size, a_o, for a range of in-service stresses based on a hypothetical fracture-mechanics life-prediction analysis for a tooth subjected to typical physiologic stresses between 5–20 MPa. Time-based lifetime estimates are based on a nominal 10^6 cycles per year.

lifetime of the tooth could be as short as several weeks, thus necessitating immediate repair.

It should be noted here that this simple fracture mechanics analysis is presented merely as an illustration of how life prediction could be performed for human teeth. Precise calculations would need to entail specific configurations of flaws and better estimates of *in vivo* stresses and stress states. We believe, however, that this approach is inherently more reliable than the traditional stress-life approach, which would not have predicted any failures for the physiologic stresses of 20 MPa. [This is so because the S/N approach does not assume the presence of pre-existing flaws, and the 20 MPa apparently is below the relevant endurance strength for dentin (Fig. 4)].

However, we have not considered several factors that may affect fatigue behavior in human dentin. These include the magnitude and physiologic loading history of the tooth, especially the presence of occasional "over-stresses" (in fact, much higher stress levels have been reported for some masticatory processes[39]); the presence of mixed-mode (tensile/compressive plus shear) loads; the physical nature of the flaws; the effect of orientation (if any) on the crack-growth rates; and the occurrence of possible long-term environmental effects on fatigue due to corrosive and bacterial fluids inside the mouth. Because of these uncertainties in the precise loading and crack size/shape configurations, the predictions made in this report must be considered only as a rough indication of the life of the tooth. However, they do indicate the general trend that for typical physiologic stresses of 5 to 20 MPa, small flaws in teeth on the order of 250 μm will not radically affect their structural integrity as predicted fatigue lifetimes will exceed the life of the patient.

CONCLUSIONS

Based on the *in vitro* study of the fatigue properties of human dentin, involving both stress/life and crack-propagation behavior in ambient temperature Hank's balanced salt solution, the following conclusions can be drawn:

1. The existence of a fatigue response to repetitive loading in human dentin tested *in vitro* has been demonstrated.
2. Attempts to discern whether the observed fatigue behavior in dentin was either cycle- and/or time-dependent, using a comparison of cyclic fatigue and sustained-load tests, were inconclusive although it appeared that both cycle- and time-dependent mechanisms were involved. Crack initiation, however, occurred far more readily under cyclic loading.
3. "Smooth-bar" stress-life (S/N) behavior for dentin was observed to exhibit "metal-like" character, with decreasing fatigue lives associated with increasing stress amplitude. S/N curves (at a load ratio of $R = 0.1$) displayed an apparent fatigue limit at 10^6–10^7 cycles, which was estimated to be ≈25 and 45 MPa, that is, ≈15 to 30% of the tensile strength, for cyclic frequencies of 2 and 20 Hz, respectively.
4. Akin to many brittle materials, the morphology of the fracture surfaces created during fatigue-crack propagation was essentially identical to those created during overload (catastrophic) failure.
5. Using a stiffness-loss technique, fatigue-crack growth rates, da/dN, for human dentin were determined from the S/N results and related to the stress-intensity range, ΔK. Resulting da/dN versus ΔK plots suggest a simple Paris power-law relationship, $da/dN \propto \Delta K^m$, with $m \approx 8.76$. Extrapolation to $\approx 10^{-10}$ m/cycle yielded an estimate of the fatigue threshold of $\Delta K_{TH} \approx 1.06$ MPa$\sqrt{}$m, that is ≈60% of the fracture toughness, K_c, of dentin.
6. A framework for a fracture-mechanics-based life-prediction methodology for the fatigue life of teeth was developed, and lifetimes projected as a function of the size of pre-existing flaws pre-

sented. Based on this preliminary analysis, it is concluded that under simulated physiologic conditions, small flaws in teeth, on the order of 250 μm, will not radically affect their structural integrity as the predicted fatigue lifetime will exceed that of the patient.

The authors thank Ms. G. Nonomura for assistance with specimen preparation, Dr. C. L. Muhlstein for helpful discussions, and EnduraTEC Inc., Minnetonka, MN, for the use of their ELF® 3200 Series testing machine.

References

1. Craig RG, Peyton FA. Elastic and mechanical properties of human dentin. J Dent Res 1958;37:710–718.
2. Lehman ML. Tensile strength of human dentin. J Dent Res 1967;46:197–201.
3. Cooper WE, Smith DC. Determination of shear strength of enamel and dentin. J Dent Res 1968;47:997.
4. Renson CE, Boyde A, Jones SJ. Scanning electron microscopy of human dentin specimens fractured in bend and torsion tests. Arch Oral Biol 1974;19:447–457.
5. Rasmussen ST, Patchin RE, Scott DB, Heuer AH. Fracture properties of human enamel and dentin. J Dent Res 1976;55: 154–164.
6. Rasmussen ST, Patchin RE. Fracture properties of human enamel and dentin in an aqueous environment. J Dent Res 1984;63:1362–1368.
7. Pashley DA, Parham P. The relationship between dentin microhardness and tubule density. Endo Dent Traumatol 1985;1: 176 –179.
8. el Mowafy OM, Watts DC. Fracture toughness of human dentin. J Dent Res 1986;65:677–681.
9. Goodis HE, Marshall GW, White JM, Gee L, Hornberger B, Marshall SJ. Storage effects on dentin permeability and shear bond strengths. Dent Mater 1993;9:79–84.
10. Sano H, Ciucchi B, Matthews WG, Pashley DH. Tensile properties of mineralized and demineralized human and bovine dentin. J Dent Res 1994;73:1205–1211.
11. Kinney JH, Balooch M, Marshall SJ, Marshall GW, Weihs TP. Hardness and Young's modulus of human peritubular and intertubular dentin. Arch Oral Biol 1996;41:9–13.
12. Watanabe L, Marshall SJ, Marshall GW. Dentin shear strength: Effects of tubule orientation and intratooth location. Dent Mater 1996;12:109–115.
13. Balooch M, Wu-Magidi IC, Balazs A, Lundkvist AS, Marshall SJ, Marshall GW, Brekhaus WJ, Kinney JH. Viscoelastic properties of dimineralized human dentin measured in water with atomic force microscope (AFM)-based indentation. J Biomed Mater Res 1998;40:539–544.
14. Povolo F, Hermida EB. Measurement of the elastic modulus of dental pieces. J Alloys Compounds 2000;310:392–395.
15. Balooch M, Demos SG, Kinney JH, Marshall GW, Balooch G, Marshall SJ. Local mechanical and optical properties of normal and transparent root dentin. J Mater Sci Mater Med 2001;12: 507–514.
16. Levitch LC, Bader JD, Shugars DA, Heymann HO. Non-carious cervical lesions. J Dent Res 1994;22:195–207.
17. Suresh S. Fatigue of materials. 2nd ed. Cambridge, U.K.: Cambridge University Press; 1998.
18. Imbeni V, Nalla RK, Bosi C, Kinney JH, Ritchie RO. On the *in vitro* fracture toughness of human dentin. J Biomed Mater Res 2003;66A:1–9.
19. Lubock P, Ritchie RO. Fatigue life estimation procedures for the endurance of a cardiac valve prosthesis: Stress/life and damage-tolerant analyses. J Biomech Eng 1986;108:153–160.
20. Ritchie RO. Fatigue and fracture of pyrolytic carbon: A damage-tolerant approach to structural integrity and life prediction in "ceramic" heart valve prostheses. J Heart Valve Dis 1996;5:S9–31.
21. White JM, Goodis HE, Marshall SJ, Marshall GW. Sterilization of teeth by gamma radiation. J Dent Res 1994;73:1560–1567.
22. Ten Cate AR. Oral histology—Development, structure and function. 4th ed. St. Louis: Mosby; 1994. p 173.
23. Vashishth D, Koontz J, Qiu S, Lundin-Cannon D, Yeni Y, Schaffler M, Fyhrie D. In vivo diffuse damage in human vertebral trabecular bone. Bone 2000;26:147–152.
24. Tada H, Paris PC, Irwin GR. 3rd ed. The stress analysis of cracks handbook. New York: ASME Press; 2000.
25. Brown WF, Srawley JE. Fracture toughness testing. In: Fracture toughness testing and its applications, ASTM STP 381. West Conshohocken, PA: American Society for Testing and Materials; 1965.
26. Jones SJ, Boyde A. Ultrastructure of dentin and dentinogenesis. In: Linde, editor. Dentin and dentinogenesis, Vol. I. Boca Raton, FL: CRC Press; 1984. p 81–134.
27. Kinney JH, Oliveira J, Haupt DL, Marshall GW, Marshall SJ. The spatial arrangement of tubules in human dentin. J Mater Sci Mater Med 2001;12:743–751.
28. Lucksanasombool P, Higgs WAJ, Higgs RJED, Swain MV. Fracture toughness of bovine bone: Influence of orientation and storage media. Biomaterials 2001;22:3127–3132.
29. Zioupos P, Currey JD, Casinos A. Tensile fatigue in bone: Are cycles-, or time to failure, or both important? J Theor Biol 2001;210:389–399.
30. Ishihara S, McEvily AJ, Goshima T, Kanekasu K, Nara T. On fatigue lifetimes and fatigue crack growth behavior of bone cement. J Mater Sci Mater Med 2000;11:661–666.
31. Ritchie RO, Dauskardt RH, Pennisi FJ. On the fractography of overload, stress corrosion and cyclic fatigue failures in pyrolytic-carbon materials used in prosthetic heart-valve devices. J Biomed Mater Res 1992;26:69–76.
32. Dauskardt RH, Ritchie RO, Takemoto JK, Brendzel AM. Cyclic fatigue and fracture in pyrolytic carbon-coated graphite mechanical heart-valve prostheses: Role of small cracks in life prediction. J Biomed Mater Res 1994;28:791–804.
33. Ritchie RO. Mechanisms of fatigue-crack propagation in ductile and brittle solids. Int J Fract 1999;100:55–83.
34. Evans AG, Fuller ER. Crack propagation in ceramic materials under cyclic loading conditions. Metallurg Trans 1974;5:27–33.
35. Evans AG, Wiederhorn SM. Proof testing of ceramic materials—An analytical basis for failure prediction. Int J Fract 1974; 10:379–392.
36. Suresh S, Ritchie RO. Mechanistic dissimilarities between environmentally-influenced fatigue crack propagation at near-threshold and higher growth rates in lower strength steels. Metal Sci 1982;16:529–538.
37. Morgan EF, Yetkinler DN, Constantz BR, Dauskardt RH. Mechanical properties of carbonated apatite bone mineral substitute: Strength, fracture and fatigue behaviour. J Mater Sci Mater Med 1997;8:559–570.
38. Wright TM, Hayes WC. The fracture mechanics of fatigue crack propagation in compact bone. J Biomed Mater Res 1976; 10:637–648.
39. Anderson DJ. Measurement of stress in mastication. I. J Dent Res 1956;35:664–670.
40. Newman JC, Raju IS. An empirical stress-intensity factor equation for the surface crack. Eng Fract Mech 1981;15:185–192.
41. Schulze KA. University of California at San Francisco; private communication; 2002.